

## PAPER

View Article Online  
View Journal | View IssueCite this: *Dalton Trans.*, 2019, **48**, 15207Received 27th August 2019,  
Accepted 16th September 2019

DOI: 10.1039/c9dt03472b

rsc.li/dalton

Synthesis and structural characterization of  
arsinoamides – early transition metal (Zr and Hf)  
and main group metal (Al, In, Sn, and Pb)  
complexes†

Xiao Chen, Michael T. Gamer and Peter W. Roesky \*

By reaction of  $MCl_4$  ( $M = Zr, Hf$ ) with 2 equiv. of  $[(Mes_2AsNPh)\{Li(OEt_2)_2\}]$ , the first group 4 metal arsinoamide complexes  $[(Mes_2AsNPh)_2MCl_2(THF)]$  were synthesized. They feature two weak  $M-As$  interactions. After formally replacing the chloride atoms by the amido ligands  $[NMe_2]^-$ , a more diverse  $M-As$  interaction arises in  $[(Mes_2AsNPh)_2M(NMe_2)_2]$ : only one  $M-As$  contact can be observed with a substantially shorter distance. This type of interaction may originate from the steric effect of the substituents on the metal center. In addition, the coordination behavior of arsinoamide in main group metal chemistry was investigated. Thus, arsinoamide complexes of  $Al(III)$ ,  $In(III)$ ,  $Sn(II)$  and  $Pb(II)$  are reported. In contrast to the group 4 complexes, no  $M-As$  interaction can be detected in these four complexes.

## Introduction

Phosphinoamides ( $R_2P-N(H)R'$ ) and their anionic derivatives  $[R_2P-NR']^-$  have been widely employed to synthesize mono- and multimetallic complexes.<sup>1–6</sup> In addition, due to the close proximity of a hard (N) and a soft donor atom (P), phosphinoamides may act as powerful ligands to investigate metal–metal interaction in the early/late heterobimetallic complexes.<sup>7–11</sup> Compared to the rich results reported for phosphinoamide-supported complexes, the coordination chemistry of their heavier arsenic analogues, arsinoamides  $[(R')_2As-NR']^-$ , is nearly unknown. Recently, we have established phenylamino (dimesityl)arsane  $Mes_2AsN(H)Ph$  ( $Mes = 2,4,6-Me_3C_6H_2$ ) and its alkali metal derivatives,  $[(Mes_2AsNPh)\{Li(OEt_2)_2\}]$ ,  $[(Mes_2AsNPh)\{Na(OEt_2)_2\}]_2$  and  $[(Mes_2AsNPh)\{K(THF)\}]_2$ .<sup>12</sup> Further reaction of lithium arsinoamide with low-valent group 14 compounds  $[(PhC(BuN)_2)ECl]$  ( $E = Si, Ge$ ),  $GeCl_2$ -dioxane led either to substitution or to  $As-N$  bond insertion products.<sup>13</sup>

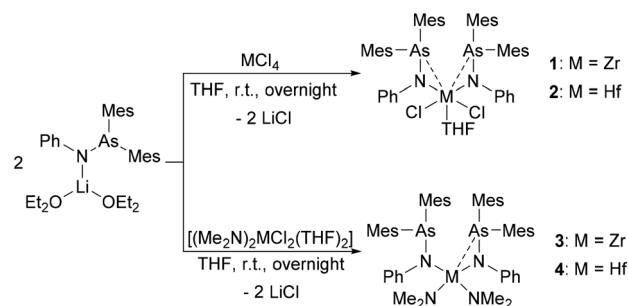
Motivated by the well-established metal complexes of phosphinoamide, we disclose here the synthesis of bi-substituted zirconium and hafnium complexes of arsinoamide. In addition, further investigation towards the substituent effect on the  $M-As$  interaction in early transition metal chemistry is

reported here. Herein, the  $Al(III)$ ,  $In(III)$ ,  $Sn(II)$  and  $Pb(II)$  complexes of arsinoamide are described.

## Results and discussion

Group 4 compounds  $[(Mes_2AsNPh)_2MCl_2(THF)]$  (**1**:  $M = Zr$  and **2**:  $M = Hf$ ) were synthesized by the reaction of  $MCl_4$  ( $M = Zr, Hf$ ) with 2 equiv. of  $[(Mes_2AsNPh)\{Li(OEt_2)_2\}]$  via a salt metathesis reaction (Scheme 1). Compounds **1** and **2** were fully characterized by standard analytical and spectroscopic techniques and the molecular structures were established by single crystal X-ray diffraction analysis.

In general, the  $^1H$  and  $^{13}C\{^1H\}$  NMR spectra of **1** and **2** show similar patterns to those observed for  $[(Mes_2AsNPh)\{Li(OEt_2)_2\}]$ . In the  $^1H$  NMR spectrum, compared to  $[(Mes_2AsNPh)\{Li(OEt_2)_2\}]$ , the resonance of the *ortho*-methyl



Scheme 1 Synthesis of compounds 1–4.

Institute of Inorganic Chemistry, Karlsruhe Institute of Technology, Engesserstr. 15, 76131 Karlsruhe, Germany. E-mail: roesky@kit.edu

†Electronic supplementary information (ESI) available: Experimental procedures, NMR and IR spectra and crystallographic studies. CCDC 1949410–1949417. For ESI and crystallographic data in CIF or other electronic format see DOI: 10.1039/C9DT03472B

groups is up-field shifted (2.30 ppm (**1**) and 2.27 ppm (**2**) vs. 2.66 ppm ( $[(\text{Mes}_2\text{AsNPh})\{\text{Li}(\text{OEt}_2)_2\}]$ ). In the  $^{13}\text{C}\{^1\text{H}\}$  NMR spectra of **1** and **2**, two signals for the methyl groups and eight aromatic signals are observed, indicating highly symmetric species of **1** and **2** in solution with equivalent aryl groups on the NMR timescale.

Single crystals suitable for X-ray diffraction analysis of **1** and **2** were obtained by slowly evaporating a dichloromethane (DCM) solution of the complexes. The crystal structures of **1** and **2** (Fig. 1) reveal isostructural complexes, which may be related to the similar atomic radii of Zr and Hf. Selected bond distances and angles are summarized in Table 1. According to the molecular structures of **1** and **2**, the M–As interaction can be observed in both compounds (Zr–As: 3.2101(6) and 3.2216(6) Å and Hf–As: 3.2423(4) and 3.2342(4) Å). Considering the longest reported bond length values (Zr–As: 2.9974 (7) Å in  $[(\text{Cp}''_2\text{Zr})\text{As}_5(\text{ZrCp}'')]$  ( $\text{Cp}'' = (\text{tBu})_2\text{C}_5\text{H}_2$ ) and Hf–As: 2.8966(7) Å in  $[\text{HfI}_4\{o\text{-C}_6\text{H}_4(\text{AsMe}_2)_2\}_2]$ ,<sup>14,15</sup> the weakness of the arsenic metal contact in **1** and **2** is evident from the longer M–As distances. We anticipate that packing effects play a significant role in these interactions. The nitrogen atoms of the arsinoamides are bound to the metal center with average distances of 2.0375 Å (Zr–N) and 2.019 Å (Hf–N), which agree with the published values for an M–N single bond (e.g. Zr–N: 2.060(3) Å and Hf–N: 2.111(4) Å).<sup>16,17</sup> The nitrogen atoms adopt a nearly

perfect planar geometry, similar to the reported electron-poor  $d^0$  metal phosphinoamide and related complexes.<sup>18–20</sup> As is apparent, the arsinoamide ligands of **1** and **2** are bound asymmetrically. In contrast to the *trans* conformation in  $[(\text{Mes}_2\text{AsNPh})\{\text{Li}(\text{OEt}_2)_2\}]$ ,<sup>12</sup> the arsinoamides in **1** and **2** exhibit a *cis* conformation, as defined by the relative orientation of the substituents on the N and As atoms. This indicates the presence of *trans* → *cis* interconversion of arsinoamide during the reaction of  $[(\text{Mes}_2\text{AsNPh})\{\text{Li}(\text{OEt}_2)_2\}]$  with  $\text{MCl}_4$ .

To further investigate the substituent effect on the M–As contact, compounds  $[(\text{Mes}_2\text{AsNPh})_2\text{M}(\text{NMe}_2)_2]$  (**3**: M = Zr and **4**: M = Hf) were synthesized by the reaction of  $[(\text{Me}_2\text{N})_2\text{MCl}_2(\text{THF})_2]$  with 2 equiv. of  $[(\text{Mes}_2\text{AsNPh})\{\text{Li}(\text{OEt}_2)_2\}]$  in a moderate yield (Scheme 1). The  $^1\text{H}$  and  $^{13}\text{C}\{^1\text{H}\}$  NMR spectra of **3** and **4** show very similar patterns. In contrast to  $[(\text{Mes}_2\text{AsNPh})\{\text{Li}(\text{OEt}_2)_2\}]$ , the resonance of the *ortho*-methyl groups of the mesityl ring is up-field shifted in the  $^1\text{H}$  NMR spectrum (2.32 ppm (**3**) and 2.31 ppm (**4**) vs. 2.66 ppm in  $[(\text{Mes}_2\text{AsNPh})\{\text{Li}(\text{OEt}_2)_2\}]$ ). A consistent trend can also be observed for the resonance of the amido ligands  $[\text{NMe}_2]^-$  (2.95 ppm (**3**) vs. 3.31 ppm in  $[(\text{Me}_2\text{N})_2\text{ZrCl}_2(\text{THF})_2]$  and 2.97 ppm (**4**) vs. 3.39 ppm in  $[(\text{Me}_2\text{N})_2\text{HfCl}_2(\text{THF})_2]$ ). Despite the fact that the M–As coordination makes the mesityl groups on As inequivalent in the solid state (*vide infra*), only one aromatic signal of the mesityl ring is detected (**3**: 6.62 ppm and **4**: 6.63 ppm). In the  $^{13}\text{C}\{^1\text{H}\}$  NMR spectrum, both complexes reveal the signals of the characteristic groups (**3**: 44.0 ( $\text{NMe}_2$ ), 22.9 (*o*-Me), and 21.0 (*p*-Me) and **4**: 43.5 ( $\text{NMe}_2$ ), 22.9(*o*-Me), and 20.9 (*p*-Me)); the observation of eight aromatic signals indicates highly symmetric species of **3** and **4** in solution.

Single crystals suitable for X-ray diffraction analysis of **3** and **4** were obtained upon cooling a diethyl ether/*n*-pentane (1/1) solution of the compounds at  $-30^\circ\text{C}$  overnight. The molecular structures of **3** and **4** reveal isostructural arrangements (Fig. 2) with the metal core lying in the center of a distorted tetrahedron with an additional M–As interaction. The metal atoms are coordinated by two nitrogen atoms of arsinoamide and two nitrogen atoms of two amido ligands. The most striking aspect of the structure is the M–As type of interaction. Only one arsenic atom is bound to the metal center (Zr–As: 3.0798(4) Å and Hf–As: 3.0892(3) Å) resulting in an  $\eta^2$  coordination mode of the corresponding arsinoamide ligand, while the other arsenic metal distances are too long to indicate a significant interaction. Despite the fact that only one M–As

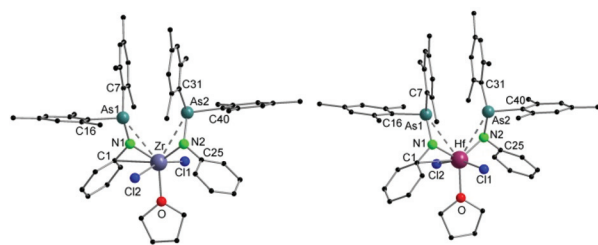


Fig. 1 Molecular structures of compounds **1** (left) and **2** (right). Hydrogen atoms and non-coordinating solvent molecules are omitted for clarity.

Table 1 Selected bond lengths (Å) and angles ( $^\circ$ ) of compounds **1**–**4**

<b>1</b>	Zr–As1	3.2101(6)	Zr–As2	3.2216(6)
	Zr–N1	2.039(4)	Zr–N2	2.036(4)
	N1–As1	1.867(3)	N2–As2	1.891(3)
	Zr–C1	2.827(5)	N1–Zr–N2	118.42(14)
<b>2</b>	Hf–As1	3.2423(4)	Hf–As2	3.2342(4)
	Hf–N1	2.020(3)	Hf–N2	2.018(3)
	N1–As1	1.870(3)	N2–As2	1.877(3)
	Hf–C1	2.794(3)	N1–Hf–N2	115.30(11)
<b>3</b>	Zr–As2	3.0798(4)	Zr–N1	2.081(2)
	Zr–N2	2.096(2)	Zr–N3	2.040(2)
	Zr–N4	2.035(2)	N1–As1	1.878(2)
	N2–As2	1.863(2)	N1–Zr–N2	118.94(7)
<b>4</b>	N3–Zr–N4	103.33(9)		
	Hf–As2	3.0892(3)	Hf–N1	2.069(2)
	Hf–N2	2.078(2)	Hf–N3	2.028(2)
	Hf–N4	2.037(3)	N1–As1	1.885(2)
	N2–As2	1.870(2)	N1–Hf–N2	118.94(9)
	N3–Hf–N4	103.67(12)		

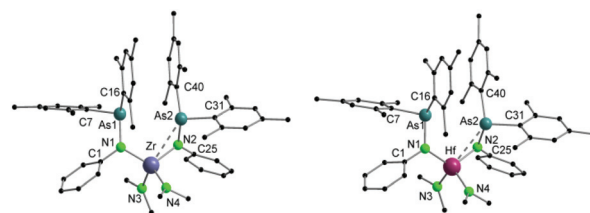


Fig. 2 Molecular structures of compounds **3** (left) and **4** (right). Hydrogen atoms are omitted for clarity.



interaction can be detected in **3** and **4**, their distances are substantially shorter (*ca.* 0.14 Å) than those in **1** and **2** (Table 1). However, packing effects may be the reason for this observation.

It should be noted that only two structurally characterized hafnium arsenic bonds were reported before:  $[(\text{Cp}'_2\text{HfCl}\{\text{AsSiMe}_3\}_2)]$  ( $\text{Cp}' = \text{MeC}_5\text{H}_3$ ) and  $[\text{HfI}_4\{o\text{-C}_6\text{H}_4(\text{AsMe}_2)_2\}_2]$ .<sup>15,21</sup> The lone pairs located on the As atoms make compounds **1–4** potentially useful as ligands for the synthesis of heterobimetallic complexes, similar to the well-known Zr(Hf) complexes of phosphinoamides.<sup>7,18,22–28</sup>

To investigate the coordination behavior of arsinoamide in main group chemistry, aluminum, indium, tin, and lead were selected as metals.

Reaction of  $\text{AlCl}_3$  with 1 equiv. of  $[(\text{Mes}_2\text{AsNPh})\{\text{Li}(\text{OEt}_2)_2\}]$  resulted, *via* a salt metathesis reaction, in the mono-substituted complex  $[(\text{Mes}_2\text{AsNPh})\text{AlCl}_2(\text{THF})]$  (**5**) (Scheme 2) in 57% crystalline yield. The  $^1\text{H}$  and  $^{13}\text{C}\{^1\text{H}\}$  NMR spectra of compound **5** are very similar to those of  $[(\text{Mes}_2\text{AsNPh})\{\text{Li}(\text{OEt}_2)_2\}]$ . For example, in the  $^1\text{H}$  NMR spectrum, the characteristic resonances of the *ortho*- and *para*-methyl groups of the mesityl ring are seen in a similar range to the starting material (2.62 ppm and 2.11 ppm in **5** vs. 2.66 ppm and 2.12 ppm in  $[(\text{Mes}_2\text{AsNPh})\{\text{Li}(\text{OEt}_2)_2\}]$ ).

Single crystals suitable for X-ray diffraction analysis of **5** were obtained by slowly evaporating a DCM solution of the complex (Fig. 3). Selected bond distances and angles are listed in Table 2. The aluminum atom coordinates to one nitrogen atom of arsinoamide, two chloride atoms, and one oxygen atom of THF, resulting in a distorted tetrahedral geometry.

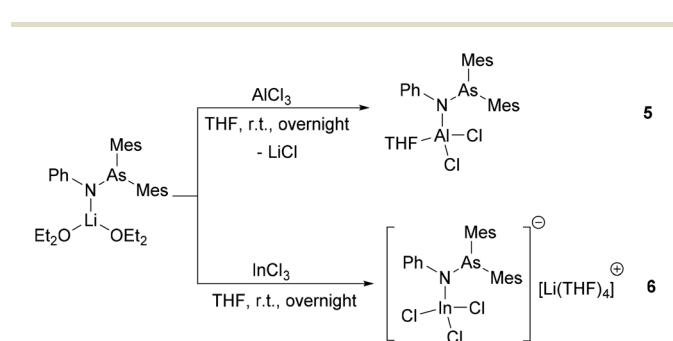
**Table 2** Selected bond lengths (Å) and angles (°) of compounds **5** and **6**

5	Al–N	1.819(3)	N–As	1.884(3)
	Al–Cl1	2.119(2)	Al–Cl2	2.1411(14)
	Al–O	1.869(3)	As–N–Al	125.9(2)
6	In–N	2.078(2)	N–As	1.861(2)
	In–Cl1	2.3884(7)	In–Cl2	2.3540(7)
	In–Cl3	2.3906(7)	As–N–In	126.33(12)

The Al–N (1.819(3) Å) and Al–O (1.869(3) Å) bond lengths are in line with the reported values (*e.g.* Al–N: 1.792(2) Å and Al–O: 1.9246(10) Å).<sup>29–31</sup> The three-coordinated nitrogen atom adopts an almost planar arrangement considering the sum of the bond angles around the nitrogen atom (357.4°). The As–N–Al bond angle (125.9(2)°) is consistent with As–N–Li (122.8(5)°) in the starting material. As seen in  $[(\text{Mes}_2\text{AsNPh})\{\text{Li}(\text{OEt}_2)_2\}]$ , arsinoamide in **5** exhibits a *trans* conformation.<sup>12</sup> No Al–As interaction can be observed in the molecular structure of **5**.

After the reaction of  $\text{InCl}_3$  with 1 equiv. of  $[(\text{Mes}_2\text{AsNPh})\{\text{Li}(\text{OEt}_2)_2\}]$  in THF,  $[(\text{Mes}_2\text{AsNPh})\text{InCl}_3][\text{Li}(\text{THF})_4]$  (**6**) was isolated in low crystalline yield, which may be explained by the instability of the product. In the  $^1\text{H}$  NMR spectrum, compared to  $[(\text{Mes}_2\text{AsNPh})\{\text{Li}(\text{OEt}_2)_2\}]$ , the resonance of the *ortho*-methyl groups is up-field shifted (2.36 ppm (**6**) vs. 2.66 ppm ( $[(\text{Mes}_2\text{AsNPh})\{\text{Li}(\text{OEt}_2)_2\}]$ )). In general, the  $^1\text{H}$  and  $^{13}\text{C}\{^1\text{H}\}$  NMR spectra of **6** show the expected pattern, which is similar to the starting material  $[(\text{Mes}_2\text{AsNPh})\{\text{Li}(\text{OEt}_2)_2\}]$ . Even under an inert atmosphere, slow decomposition of **6** was observed at room temperature, resulting in the formation of aminoarsane ( $\text{Mes}_2\text{AsN}(\text{H})\text{Ph}$ ). In the  $^1\text{H}$  NMR spectrum, the characteristic resonances of the *ortho*-, *para*-methyl (2.35 and 2.06 ppm, respectively) and NH groups (3.99 ppm), with an integral ratio of 12:6:1, can be detected, which are assigned to  $[\text{Mes}_2\text{AsN}(\text{H})\text{Ph}]$  (Fig. S19†). In the IR spectrum, a single N–H stretching absorption band at  $3376\text{ cm}^{-1}$  further proves the formation of  $[\text{Mes}_2\text{AsN}(\text{H})\text{Ph}]$  ( $3377\text{ cm}^{-1}$ ) (Fig. S28†). A similar decomposition has been reported during the reaction of phosphinoamide lanthanide complexes  $[(\text{Ph}_2\text{PNPh})_4\text{Ln}][\text{Li}(\text{THF})_4]$  ( $\text{Ln} = \text{Y}, \text{Lu}$ ) with  $[\text{Pd}_2(\text{C}_3\text{H}_5)_2\text{Cl}_2]$ , where the neutral aminophosphine  $[\text{Ph}_2\text{PN}(\text{H})\text{Ph}]$  was formed.<sup>10</sup>

Single crystals suitable for X-ray diffraction analysis of **6** were obtained by slowly evaporating a THF solution of the complex (Fig. 3). Single crystal X-ray diffraction analyses reveal that **6** is composed of a  $[\text{Li}(\text{THF})_4]^+$  cation and a  $[(\text{Mes}_2\text{AsNPh})\text{InCl}_3]^-$  anion. The indium atom is four-coordinated by three chloride and one nitrogen atoms of arsinoamide, resulting in a distorted tetrahedral geometry. The three-coordinated nitrogen atom adopts a nearly perfect planar trigonal geometry (the sum of bonding angles:  $359.3^\circ$ ). The N–As bond distance (1.861(2) Å) does not deviate significantly from  $[(\text{Mes}_2\text{AsNPh})\{\text{Li}(\text{OEt}_2)_2\}]$  (1.816(6) Å). However, the As–N–M bond angle (As–N–In:  $126.33(12)^\circ$ ) is larger than that in  $[(\text{Mes}_2\text{AsNPh})\{\text{Li}(\text{OEt}_2)_2\}]$  (As–N–Li:  $112.8(5)^\circ$ ). No In–As interaction can be observed in the molecular structure of **6**. To the best of our knowledge no comparable structurally characterized indium phosphinoamide complex is known so far.



**Scheme 2** Synthesis of compounds **5** and **6**.

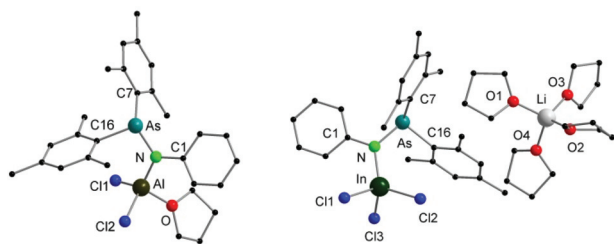
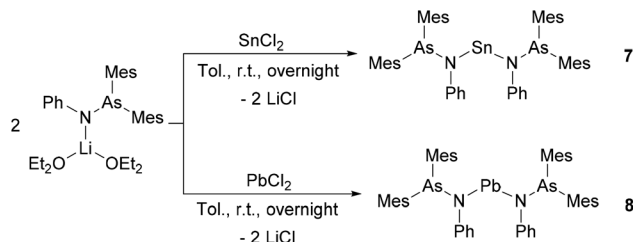


**Fig. 3** Molecular structures of compounds **5** (left) and **6** (right). Hydrogen atoms are omitted for clarity.





Scheme 3 Synthesis of compounds 7 and 8.

Encouraged by the attractive reactivity of silylene and germylene with arsinoamide,<sup>13</sup> the heavier homoleptic bi-substituted complexes of stannylene and plumbylene,  $[(\text{Mes}_2\text{AsNPh})_2\text{E}]$  ( $\text{E} = \text{Sn}$  (7) and  $\text{Pb}$  (8)), were isolated by the reaction of  $\text{ECl}_2$  with 2 equiv. of  $[(\text{Mes}_2\text{AsNPh})\{\text{Li}(\text{OEt})_2\}]$  (Scheme 3).

Compound 8 is extremely sensitive towards moisture and oxygen. In the solid state, compounds 7 and 8 are stable at room temperature under an inert atmosphere. Nevertheless, slow decomposition can be detected in  $\text{C}_6\text{D}_6$  at room temperature. Compounds 7 and 8 show very similar patterns in the  $^1\text{H}$  and  $^{13}\text{C}\{^1\text{H}\}$  NMR spectra as observed for  $[(\text{Mes}_2\text{AsNPh})\{\text{Li}(\text{OEt})_2\}]$ . In the  $^{119}\text{Sn}\{^1\text{H}\}$  NMR spectrum, the resonance of 7 is detected at 319 ppm, which is in line with that at 291 ppm for N-heterocyclic stannylene  $[\{\text{CH}_2(\text{CH}_2\text{NDipp})_2\}\text{Sn}]$ .<sup>32</sup> The  $^{207}\text{Pb}\{^1\text{H}\}$  NMR signal of 8 (3244 ppm) is in the range of reported diamido plumbylene complexes (e.g. 3504 ppm in  $[\{\text{DippN}(\text{CH}_2)_3\text{NDipp}\}\text{Pb}]$ ).<sup>33</sup>

Single crystals of both 7 and 8 were grown by diffusion of a mixture of *n*-pentane and diethyl ether (1/1) into a solution of the complexes in toluene (Fig. 4). Single crystal X-ray diffraction analyses reveal that both compounds are isostructural. They crystallize in the tetragonal space group  $I4_1/a$ . Selected bond lengths and angles are listed in Table 3.

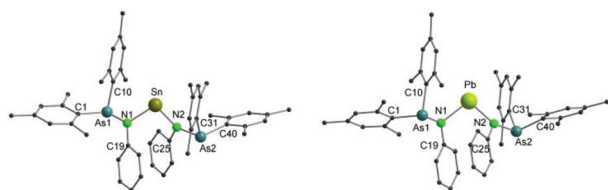


Fig. 4 Molecular structures of 7 (left) and 8 (right). Hydrogen atoms are omitted for clarity.

Table 3 Selected bond lengths (Å) and angles (°) of compounds 7 and 8

7	Sn–N1	2.120(4)	Sn–N2	2.115(4)
	N1–As1	1.880(4)	N2–As2	1.880(4)
	N1–Sn–N2	97.8(2)		
8	Pb–N1	2.236(6)	Pb–N2	2.211(6)
	N1–As1	1.872(6)	N2–As2	1.873(6)
	N1–Pb–N2	97.4(2)		

In both 7 and 8, the central metal atom is coordinated by two nitrogen atoms of the arsinoamide ligands. The E–N bond distances (Sn–N: 2.115(4) and 2.120(4) Å and Pb–N: 2.211(6) and 2.236(6) Å) fit well to the published values for the E–N single bond (e.g. 2.089(2) Å and 2.115(2) Å (Sn–N) and 2.087(5) Å and 2.298(4) Å (Pb–N)).<sup>33–36</sup> The N–E–N bond angles (N1–Sn–N2: 97.8(2)° and N1–Pb–N2: 97.4(2)°) are smaller than the comparable N–E–N bond angles (e.g. 106.13(8)° and 104.7(2)° (N–Sn–N) and 100.60(8)° and 105.75(14)° (N–Pb–N)),<sup>37–39</sup> which may originate from the steric effect of the ligand. The sum of bond angles around the nitrogen atoms varies from 348.9° to 356.4°, indicating a slightly disordered pyramidal geometry of the nitrogen atoms. None of the arsenic atoms shows any interaction with the metal center in 7 and 8. To the best of our knowledge, there is no comparable structurally characterized stannylene or plumbylene complexes of phosphinoamides.

## Conclusions

In summary, the reaction of arsinoamide with early transition metals (Zr(IV) and Hf(IV)) and main group metals (Al(III), In(III), Sn(II) and Pb(II)) was investigated. In the case of Zr and Hf, di(arsinoamide) complexes 1–4 were established, in which the first  $\eta^2$  coordination mode of arsinoamide can be observed. In addition, it seems that the packing effects can significantly influence the M–As interaction. Due to the presence of the As lone pair, compounds 1–4 can act as potentially useful ligands for further synthesis of early/late heterobimetallic complexes. In the arsinoamide main group metal complexes of Al(III), In(III), Sn(II), and Pb(II) only the nitrogen atom binds to the metal center. The lone pair on As remains uncoordinated.

## Conflicts of interest

There are no conflicts to declare.

## Acknowledgements

X. C. thanks the China Scholarship Council (No. 201506250062) for generous support. Financial support provided by the DFG-funded transregional collaborative research center SFB/TRR 88 “Cooperative Effects in Homo and Heterometallic Complexes (3MET)”, projects B3 is acknowledged.

## Notes and references

- Z. Fei and P. J. Dyson, *Coord. Chem. Rev.*, 2005, **249**, 2056–2074.
- P. W. Roesky, *Heteroat. Chem.*, 2002, **13**, 514–520.
- C. Fliedel, A. Ghisolfi and P. Braunstein, *Chem. Rev.*, 2016, **116**, 9237–9304.





- 4 H. Zhang, G. P. Hatzis, C. E. Moore, D. A. Dickie, M. W. Bezpalko, B. M. Foxman and C. M. Thomas, *J. Am. Chem. Soc.*, 2019, **141**, 9516–9520.
- 5 A. Stasch, *Dalton Trans.*, 2014, **43**, 7078–7086.
- 6 A. J. Ayres, M. Zegke, J. P. Ostrowski, F. Tuna, E. J. McInnes, A. J. Woolees and S. T. Liddle, *Chem. Commun.*, 2018, **54**, 13515–13518.
- 7 H. Zhang, B. Wu, S. L. Marquard, E. D. Litle, D. A. Dickie, M. W. Bezpalko, B. M. Foxman and C. M. Thomas, *Organometallics*, 2017, **36**, 3498–3507.
- 8 F. Völcker and P. W. Roesky, *Dalton Trans.*, 2016, **45**, 9429–9435.
- 9 M. J. Sgro and D. W. Stephan, *Chem. Commun.*, 2013, **49**, 2610–2612.
- 10 F. Völcker, F. M. Mück, K. D. Vogiatzis, K. Fink and P. W. Roesky, *Chem. Commun.*, 2015, **51**, 11761–11764.
- 11 C. M. Thomas, J. W. Napoline, G. T. Rowe and B. M. Foxman, *Chem. Commun.*, 2010, **46**, 5790–5792.
- 12 X. Chen, M. T. Gamer and P. W. Roesky, *Dalton Trans.*, 2018, **47**, 12521–12525.
- 13 X. Chen, T. Simler, R. Yadav, M. T. Gamer, R. Köppe and P. W. Roesky, *Chem. Commun.*, 2019, **55**, 9315–9318.
- 14 M. Schmidt, A. E. Seitz, M. Eckhardt, G. B. Balázs, E. V. Peresyphkina, A. V. Virovets, F. Riedlberger, M. Bodensteiner, E. M. Zolnhofer, K. Meyer and M. Scheer, *J. Am. Chem. Soc.*, 2017, **139**, 13981–13984.
- 15 W. Levason, M. L. Matthews, B. Patel, G. Reid and M. Webster, *Dalton Trans.*, 2004, 3305–3312.
- 16 L. N. Grant, M. E. Miehllich, K. Meyer and D. J. Mindiola, *Chem. Commun.*, 2018, **54**, 2052–2055.
- 17 L. Grocholl, L. Stahl and R. J. Staples, *Chem. Commun.*, 1997, 1465–1466.
- 18 B. G. Cooper, C. M. Fafard, B. M. Foxman and C. M. Thomas, *Organometallics*, 2010, **29**, 5179–5186.
- 19 H. Nagashima, T. Sue, T. Oda, A. Kanemitsu, T. Matsumoto, Y. Motoyama and Y. Sunada, *Organometallics*, 2006, **25**, 1987–1994.
- 20 M. A. Rankin and C. C. Cummins, *Dalton Trans.*, 2012, **41**, 9615–9618.
- 21 F. Lindenberg, J. Sieler, E. Hey-Hawkins, U. Müller and A. Pilz, *Z. Anorg. Allg. Chem.*, 1996, **622**, 683–688.
- 22 T. Sue, Y. Sunada and H. Nagashima, *Eur. J. Inorg. Chem.*, 2007, **2007**, 2897–2908.
- 23 Y.-T. Bi, L. Li, Y.-R. Guo and Q.-J. Pan, *Inorg. Chem.*, 2019, **2**, 1290–1300.
- 24 C. M. Thomas, *Comments Inorg. Chem.*, 2011, **32**, 14–38.
- 25 J. P. Krogman and C. M. Thomas, *Chem. Commun.*, 2014, **50**, 5115–5127.
- 26 W. Zhou, N. I. Saper, J. P. Krogman, B. M. Foxman and C. M. Thomas, *Dalton Trans.*, 2014, **43**, 1984–1989.
- 27 N. I. Saper, M. W. Bezpalko, B. M. Foxman and C. M. Thomas, *Polyhedron*, 2016, **114**, 88–95.
- 28 H. Zhang, G. P. Hatzis, C. E. Moore, D. A. Dickie, M. W. Bezpalko, B. M. Foxman and C. M. Thomas, *J. Am. Chem. Soc.*, 2019, **141**, 9516–9520.
- 29 K. J. Blakeney, P. D. Martin and C. H. Winter, *Dalton Trans.*, 2018, **47**, 10897–10905.
- 30 H. S. Zijlstra, J. Pahl, J. Penafiel and S. Harder, *Dalton Trans.*, 2017, **46**, 3601–3610.
- 31 T. Agou, T. Wasano, T. Sasamori and N. Tokitoh, *Organometallics*, 2014, **33**, 6963–6966.
- 32 S. M. Mansell, C. A. Russell and D. F. Wass, *Inorg. Chem.*, 2008, **47**, 11367–11375.
- 33 J. P. Charmant, M. F. Haddow, F. E. Hahn, D. Heitmann, R. Fröhlich, S. M. Mansell, C. A. Russell and D. F. Wass, *Dalton Trans.*, 2008, 6055–6059.
- 34 J. A. Cabeza, J. M. Fernández-Colinas, P. García-Álvarez and D. Polo, *Inorg. Chem.*, 2012, **51**, 3896–3903.
- 35 S. I. Al-Rafia, P. A. Lummis, M. J. Ferguson, R. McDonald and E. Rivard, *Inorg. Chem.*, 2010, **49**, 9709–9717.
- 36 M. Chen, J. R. Fulton, P. B. Hitchcock, N. C. Johnstone, M. F. Lappert and A. V. Protchenko, *Dalton Trans.*, 2007, 2770–2778.
- 37 T. J. Hadlington, J. A. Abdalla, R. Tirfoin, S. Aldridge and C. Jones, *Chem. Commun.*, 2016, **52**, 1717–1720.
- 38 T. Fjeldberg, H. Hope, M. F. Lappert, P. P. Power and A. J. Thorne, *J. Chem. Soc., Chem. Commun.*, 1983, 639–641.
- 39 M. Aman, O. Mrózek, L. Dostál, Z. Růžicková and R. Jambor, *J. Organomet. Chem.*, 2018, **872**, 1–7.

